More extreme swings of the South Pacific Convergence Zone due to greenhouse warming

Wenju Cai[1], Matthieu Lengaigne[2], Simon Borlace[1], Mat Collins[3], Tim Cowan[1], Michael J. McPhaden[4], Axel Timmermann[5], Scott Power[6], Josephine Brown[6], Christophe Menkes[7], Arona Ngari[8], Emmanuel M. Vincent[2], and Matthew J. Widlansky[9]

1. CSIRO Marine and Atmospheric Research, Aspendale, Victoria, Australia
2. Laboratoire d'Océanographie et du Climat: Expérimentation et Approches Numériques (LOCEAN), IRD/UPMC/CNRS/MNHN, Paris, France
3. College of Engineering Mathematics and Physical Sciences, Harrison Building, Streatham Campus, University of Exeter, Exeter, UK and Met Office Hadley Centre, FitzRoy Road, Exeter, EX1 3PB, UK,
4. NOAA/Pacific Marine Environmental Laboratory, Seattle, Washington 98115, USA
5. IPRC, Department of Oceanography, SOEST, University of Hawaii, Honolulu, Hawaii 96822, USA
6. Centre for Australian Weather and Climate Research, Bureau of Meteorology, Melbourne, Victoria, Australia
7. Institut de Recherche pour le Développement, Noumea, New Caledonia
8. Meteorological Service, Avarua, Rarotonga, Cook Islands
9. International Pacific Research Center, University of Hawaii at Manoa, Honolulu, Hawaii 96822, USA

Wenju Cai: Wenju.Cai@csiro.au

Matthieu Lengaigne: Matthieu.Lengaigne@locean-ipsl.upmc.fr

Simon Borlace: Simon.Borlace@csiro.au

Mat Collins: M.Collins@exeter.ac.uk

Tim Cowan: Tim.Cowan@csiro.au

Michael J. McPhaden: michael.j.mcphaden@noaa.gov

Axel Timmermann: axel@hawaii.edu

Scott Power: S.Power@bom.gov.au

Josephine Brown: J.Brown@bom.gov.au

Christophe Menkes: christophe.menkes@ird.fr

Arona Ngari: angari@oyster.net.ck

Emmanuel Vincent: emmanuel.vincent@locean-ipsl.upmc.fr

Matthew Widlansky: mwidlans@hawaii.edu

The South Pacific convergence zone (SPCZ) is the Southern Hemisphere's most expansive and persistent rain band, extending from the equatorial western Pacific southeastward toward French Polynesia[1-2]. Due to its strong rainfall gradient, a small displacement in the SPCZ's position causes drastic changes to hydroclimatic conditions and the frequency of extreme weather events such as droughts, floods and tropical cyclones experienced by vulnerable island countries in the region[1-7]. The SPCZ position varies from its climatological mean location with the El Niño-Southern Oscillation (ENSO), moving a few degrees northward during moderate El Niño events and southward during La Niña events[2,5,6]. During strong El Niño events, however, the SPCZ undergoes an extreme swing of up to 10 degrees to the equator and collapses to a more zonally oriented structure[5] with commensurately severe impacts[5,8-11]. Understanding changes in the characteristics of the SPCZ in a changing climate is therefore of broad scientific and socioeconomic interest. Here we show climate modelling evidence for a near doubling in the occurrences of zonal SPCZ events from 1891-1990 to 1991-2090 in response to greenhouse warming, even in the absence of a consensus on how itself ENSO will change[12-14]. We estimate the increase in zonal SPCZ events from an aggregation of the climate models in the Coupled Model Intercomparison Project phases 3 and 5 (CMIP3[15] and CMIP5) multi-model database that are able to simulate such events. The change is caused by a projected enhanced equatorial warming in the Pacific[16] and may lead to more frequent occurrences of extreme events across the Pacific Island nations most affected by zonal SPCZ events.

The SPCZ plays a significant role in global circulation and is a major feature of the Southern Hemisphere's climate[1,2]. Its location largely controls rainfall, ocean circulation and tropical cyclogenesis patterns in the South Pacific[5-7]. The western, more equatorial portion of the SPCZ rainfall band is largely controlled by sea surface temperature (SST), while its eastern portion is also influenced by extra-tropical circulation and the subtropical dry zone of the south-eastern Pacific[1,17]. As the SPCZ moves north-eastward during El Niño events, countries located within the climatological SPCZ position experience forest fires and droughts[3,4] as well as an increased probability of tropical cyclone hits[5]. In addition, the associated environmental changes affect fisheries[18] and cause coral reef mortality through

thermally-induced coral bleaching[8-11] across the South Pacific. Observed zonal SPCZ events, characterized by a collapse of the meridional tilt of the rain band, often associated with an equatorward shift of intertropical convergence zone, have occurred in conjunction with the strongest recorded El Niño events (e.g., 1982/83, 1997/98). The impacts from these zonal SPCZ events are much more severe than those from weaker El Niño events, and include massive drought and food shortage[7], unprecedented coral bleaching-induced mortality[9,10] and cyclogenesis in the vicinity of French Polynesia[5], a region not accustomed to such occurrences.

These dramatic impacts raise the question as to whether greenhouse warming will change the frequency of zonal SPCZ events. Although many studies have addressed the effects of a projected warming on the Pacific mean state[13,14,19,20], ENSO and its multiplicity[12-14,21,22], and the mean position of the SPCZ[23], the issue of how zonal SPCZ events will change in a warming climate has received little attention. Here we show that greenhouse warming leads to a significant increase in the frequency of such events.

We apply a multivariate signal processing method referred to as Empirical Orthogonal Function (EOF) analysis to deconvolve the spatio-temporal rainfall variability into orthogonal modes, each described by a principal spatial pattern and an associated principal component time series[24]. For observations, we use the satellite-era rainfall dataset[25] focusing on austral summer (December to February) when the SPCZ is best developed. The leading pattern (Fig. 1a) features opposite rainfall anomalies between the equatorial and south-western Pacific around the climatological rain band position. The second pattern (Fig. 1b) is characterized by opposite rainfall anomalies in the equatorial western and central Pacific.

A nonlinear relationship exists between the two associated principal components (time series). In one cluster of events, the principal components are negatively correlated (blue, green, and black dots; Fig. 1c) and rainfall anomalies embedded in the two patterns tend to offset each other east of the dateline, resulting in rainfall variability located in the western Pacific. This cluster indeed encompasses years characterized by the well-known northward and southward shift of the SPCZ during La Niña and moderate El Niño events, respectively (blue and green lines; Fig. 1a). In

the second cluster, the principal components are both positive (red dots; Fig. 1c) and display a positive correlation, resulting in large precipitation anomalies east of the dateline. This cluster consists of the three reported zonal SPCZ events[5] (1982/83, 1991/1992, and 1997/98, or one in 11 years) where the eastern portion moves equatorward by more than 10° in latitude (red line; Fig. 1b). A nonlinear relationship of the second principal component with a historical ENSO index (e.g., Niño3.4) is apparent (Supplementary Fig. 1), although we do not distinguish the canonical from the Modoki[22] ENSO. We define a zonal SPCZ event as one for which the first principal component is greater than a one standard deviation value and the second principal component is greater than zero.

We use this nonlinear behaviour to benchmark the performance of 17 coupled general circulation models (CGCM) from the CMIP3[15] database forced with historical anthropogenic and natural forcings before year 2000, and greenhouse gas emission scenario (SRESA2)[15] after year 2000. Nine models fail this test (Supplementary Fig. 2). We focus on eight CGCMs that realistically simulate the two principal spatial patterns of rainfall anomalies (Figs. 2a and 2b), the nonlinear behaviour between the associated principal components (Figs. 2c and 2d), and the relationship with ENSO (Supplementary Figs. 3 and 4). We compare the frequency of zonal SPCZ events in the first (1891-1990) and second (1991-2090) 100-year periods, referred to as the *Control* and *Climate Change* periods, respectively, to investigate the influence of greenhouse warming.

Aggregated over these eight CMIP3 CGCMs, the frequency of zonal SPCZ events increases by 81%, from about one event every 14 years in the *Control* period to one every 7-8 years in the *Climate Change* period (Figs. 2c and 2d). This is statistically significant above the 95% confidence level based on a bootstrap test[26]. The statistical significance is underscored by a strong consensus among CGCMs, with six out of eight models simulating an increase in occurrences; a sensitivity test to varying definitions of zonal SPCZ events supports the robustness of our result (Supplementary Fig. 3 and Table 1).

An identical analysis is conducted on rainfall outputs of 35 available experiments from 20 CMIP5 CGCMs under the historical and a Representative Concentration Pathway (RCP8.5) scenario. Aggregated over 15 experiments from eight CMIP5 CGCMs that reproduce the nonlinear behaviour of the SPCZ, there is a similar increase in the occurrences of zonal SPCZ events, from one every 16 years in the *Control* period to one every 7.5 years in the *Climate Change* period (Supplementary Table 2 and Fig. 5).

We assess the potential impact of well-known biases in simulated climatological SST and SPCZ[23] using the HadCM3 CGCM, in which biases are corrected through a fixed flux adjustment[13], in a set of 17 perturbed physics ensemble (PPE) climate change experiments forced with a 1% per year CO_2 increase. In these PPE experiments, perturbations are made to uncertain physical parameters within a single model structure. Aggregated over 12 experiments that produce the nonlinear behaviour of the SPCZ, there is a 214% increase in the frequency of zonal SPCZ events from one event every 21 years in the *Control* period to one event every 7 years in the *Climate Change* period (Supplementary Fig. 6 and Table 3). Thus, the conclusions drawn from CMIP3 and CMIP5 CGCMs are not a consequence of the SST biases.

Understanding the relationship between the SPCZ and SST anomalies is crucial for unravelling the mechanism of the increase in zonal SPCZ events in a warming climate. To achieve this, modelled SST, wind and rainfall composite patterns are obtained for zonal SPCZ events (Fig. 3). In both periods, an eastward extension of the Pacific warm pool results in a substantial decrease of the meridional SST gradient south of the equator, with a rainfall reduction over the western Pacific including northern Australia. In response, eastward-shifted westerly anomalies develop, with a maximum east of the dateline and south of the equator, accompanied by strong south-easterlies south of the warm SST anomalies (Figs. 3a and 3b), as in the observed[5, 27-28]. Such a wind response increases the moisture convergence east of the dateline and south of the equator, displacing the maximum moisture convergence and precipitation axis by up to 10° latitude to the north from its climatological position and contributing to the zonal orientation of the SPCZ (Figs. 3c and 3d). A zonal SPCZ event therefore occurs when the equatorial western Pacific moves from a state in

which the off-equatorial region is warmer than the equatorial region to a condition in which the meridional SST gradient (the off-equatorial minus the equatorial) decreases considerably (Supplementary Figs. 7 and 8). An increase in the frequency of zonal SPCZ events may hence arise from more frequent occurrences of a vanishing meridional SST gradient, which may be associated with a change in the occurrences of strong El Niño events. This mechanism also operates for the CMIP5 models for which data are available at the time of writing.

As shown in Supplementary Fig. 9, climate change induces a larger warming rate along the equator than in the off-equatorial central Pacific, a common feature of the response to global warming[16,29-30]. This pattern results in a slight decrease of the climatological meridional SST gradient in the central Pacific, which translates to an increase in the frequency of austral summers where the meridional SST gradient diminishes (e.g., <0.25°C, Fig. 4a). Such a change occurs in all eight CMIP3 CGCMs (Fig. 4b), and in aggregation, the number of austral summers with a vanishing meridional SST gradient (i.e., < 0.25°C) increases by 140%, from one every 15 summers during the *Control* period to one every six summers during the *Climate Change* period. In association, for a given vanishing meridional SST gradient, the number of zonal SPCZ events increases (Fig. 4c).

In addition, there is a 32% increase in strong El Niño events (as measured by a Niño3.4 greater than a 1.5-standard deviation value; Supplementary Table 3). This increase, seen in five out of eight CMIP3 CGCMs (Figure 4d), occurs despite a tendency for a decrease in the total number of El Niño events (defined as when Niño3.4 is greater than a 0.5 or 0.75 standard deviation value), and despite a general lack of consensus on how the El Niño amplitude may change[12,13]. However, only about 50% of the total increase in zonal SPCZ events coincides with a strong El Niño event, suggesting that such a change in El Niño is not necessary for an increase in zonal SPCZ events. Indeed, results from the 12 PPE experiments show a lack of consensus among experiments and an overall decrease in the frequency of strong El Niño events, despite a large increase in the frequency of zonal SPCZ events (Supplementary Fig. 10 and Table 5), highlighting the fundamental importance of a decrease in the meridional SST gradient.

In summary, increased occurrences of zonal SPCZ events are consistent with the background state change in SST, and support our conclusion of an association with human-induced global warming. The increase is generated despite a lack of consensus on a definitive response of ENSO to greenhouse warming. With this increase, we expect more frequent occurrences of extreme events such as droughts, floods, and tropical cyclones in the Pacific Island nations most affected by zonal SPCZ events.

METHODS SUMMARY

The zonal SPCZ events were diagnosed from observations and CGCMs. We propose an identification method based on the historical events, in which we apply EOF analysis to the satellite era austral summer rainfall anomalies for the 1979-2008 period over the South Pacific domain (160^{o}E-80^{o}W, Eq.-30^{o}S). The rainfall anomalies are referenced to the climatological mean of the full period. This yields two leading patterns, one reflecting opposite rainfall anomalies between the equatorial and south-western Pacific around the climatological rain band position, the other characterised by opposite rainfall anomalies in the equatorial western and central Pacific. The outputs of the analysis are arranged so that the principal component time series have a standard deviation of one, and the differences in variance are expressed in the pattern. Anomalies beyond the South Pacific domain are obtained by a linear regression. A zonal SPCZ event is defined as when the first leading time series is greater than one standard deviation, and when the second leading time series is positive. This definition captures the three observed zonal SPCZ events in the second cluster. We also test the sensitivity of our results to varying definitions (Supplementary Table 1). The method is applied to rainfall anomalies of 17 CMIP3 CGCM simulations, each covering 110 years of a pre-21st century climate change simulation using historical anthropogenic and natural forcings (1891-2000) and another 90 years (2001-2090; the longest common period for the CGCMs) from a future greenhouse warming simulation using the A2 greenhouse gas emission scenario (SRESA2)[15]. The same method is applied to 35 CMIP5 experiments under historical anthropogenic and natural forcings and the RCP8.5

forcing scenario, and 17 PPE experiments forced with historical and a 1% per year CO_2 increase, covering a 200-year period.

References

1. Kiladis, G. N., Storch, H. V. & Loon, H. V. Origin of the South Pacific convergence Zone. *J. Clim.* **2**, 1185–1195 (1988).
2. Vincent, D. G. The south Pacific convergence zone (SPCZ): a review. *Mon. Weather Rev.* **122,** 1949–1970 (1994).
3. Salinger, M. J., Renwick, J. A. & Mullan, A. B. Interdecadal Pacific oscillation and South Pacific climate. *Int. J. Climatol.* **21**, 1705–1721 (2001)
4. Kumar, V. V., Deo R. C. & Ramachandran V. Total rain accumulation and rain-rate analysis for small tropical Pacific islands: a case study of Suva, Fiji. *Atmos. Science Lett*. **7**, 53-58 (2006).
5. Vincent, E. M. *et al*. Interannual variability of the South Pacific convergence zone and implications for tropical cyclone genesis. *Clim. Dyn.* **36**, 1881-1896 (2011).
6. Folland, C. K., Renwick, J. A., Salinger, M. J. & Mullan, A. B. Relative influence of the interdecadal Pacific oscillation and ENSO on the South Pacific Convergence Zone. *Geophys. Res. Lett.* **29:**1643. doi:10.1029/2001GL014201 (2002).
7. *Australian Bureau of Meteorology and CSIRO, 2011:* Climate change in the Pacific: Scientific Assessment and New Research. *Volume 1: Regional Overview. Volume 2: Country Reports. Scientific Editors: K. Hennessy, S. Power and G. Cambers.*
8. Barnett, J. Dangerous climate change in Pacific Islands: *food production and food security. Reg. Environ. Change* **11**, 229-237 (2011).
9. Glynn P. Widespread coral mortality and the 1982-83 El Niño warming event. *Envir. Conservation,* **11**, 133-146 (1984).
10. Hoegh,-Guldberg O. Climate change, coral beaching and the future of the world's coral reefs. *Mar. Freshwater Res*. **50**, 839-866 (1999).
11. Mumby P.J. *et al*. Unprecedented bleaching-induced mortality in Porites spp. at Rangiroa Atoll, French Polynesia, *Marine Biology* **139**, 183-189 (2001).

12. Guilyardi, E. et al. Understanding El Niño in ocean–atmosphere general circulation models: progress and challenges. *Bull. Am. Meteorol. Soc.* **90**, 325–340 (2009).
13. Collins, M. et al. The impact of global warming on the tropical Pacific Ocean and El Niño. *Nature Geoscience* **3**, 391 - 397 (2010).
14. Ashok, K., Sabin, T. P., Swapna, P., and Murtugudde, R. G. Is a global warming signature emerging in the tropical Pacific?, *Geophys. Res. Lett.* **39,** L02701, doi:10.1029/2011GL050232 (2012).
15. Meehl, G. *et al*. The WCRP CMIP3 multimodel Dataset: A New Era in Climate Change Research. *Bull. Amer. Meteor. Soc.* **88**, 1383-1394 (2007).
16. Xie, S. P. *et al*. Global Warming Pattern Formation: Sea Surface Temperature and Rainfall. *J. Clim.* **23**, 966-986 (2010).
17. Takahashi, K. & Battisti, D. S. Processes controlling the mean tropical Pacific precipitation pattern. Part II: the SPCZ and the southeast Pacific dry zone. *J. Clim.* **20,** 5696–5706 (2007).
18. Lehodey, P., Bertignac, M., Hampton, J., Lewis, A. and Picaut, J. El Niño Southern Oscillation and tuna in the western Pacific. *Nature* **389**, 715–718 (1997).
19. Cane, M. A. et al. Twentieth-Century Sea Surface Temperature Trends. *Science 275,* 957-960 (1997).
20. Vecchi, G. A. et al. Weakening of tropical Pacific atmospheric circulation due to anthropogenic forcing. *Nature* 441, 73–76 (2006).
21. Yeh, S.-W. et al. El Niño in a changing climate. Nature, 461, 511–514 (2009).
22. Ashok, K., Behera, S. K., Rao, S. A., Weng, H. & Yamagata, T. El Niño Modoki and its possible teleconnection. *J. Geophys. Res.* **112,** C11007, doi:10.1029/2006JC003798 (2007).
23. Brown, J. R., Moise, A. F., and Delage, F. P. Changes in the South Pacific Convergence Zone in IPCC AR4 future climate projections. *Clim. Dyn.* in press.
24. Lorenz, E. N., Empirical orthogonal functions and statistical weather prediction. MIT Department of Meteorology, Statistical Forecast Project Rep. 1, 49 pp. (1956) [Available from Dept. of Meteorology, MIT, Massachusetts Ave., Cambridge, MA 02139.]

25. Adler, R. F. et al. The version 2 Global Precipitation Climatology Project (GPCP) monthly precipitation analysis (1979-present). *J. Hydrometeor.* **4**, 1147–1167 (2003).
26. Austin, P. C. Bootstrap Methods for Developing Predictive Models. *The American Statistician* **58,** 131-137 (2004).
27. Spencer, H. Role of the atmosphere in seasonal phase locking of El Niño. *Geophys. Res. Lett.* **31**:L24104 (2004).
28. Lengaigne, M., Boulanger, J. P., Menkes, C. & Spencer, H. Influence of the seasonal cycle on the termination of El Niño events in a coupled general circulation model. *J. Clim.* **19**, 1850–1868 (2006).
29. Liu, Z., Vavrus, S., He, F., Wen, N. & Zhong, Y. Rethinking tropical ocean response to global warming: The enhanced equatorial warming. *J. Clim.* **18,** 4684–4700 (2005).
30. Timmermann, A., McGregor, S. & Jin, F.-F. Wind effects on past and future regional sea level trends in the southern Indo-Pacific. *J. Clim.* **23,** 4429–4437 (2010).

Figure Captions

Figure 1| Principal variability patterns of observed rainfall and their nonlinear relationship. a and **b**, Spatial patterns obtained by applying a statistical and signal processing method, Empirical Orthogonal Function analysis[24], to a satellite-era rainfall dataset from the Global Precipitation Climatology Project version 2[25], focusing on the South Pacific domain (Eq.-30°S, 160°E-80°W) and the SPCZ prevailing season of austral summer (December to February). The associated pattern beyond the domain is obtained by linearly regressing rainfall anomalies onto the time series. The first and second principal spatial patterns account for 47% and 16% of the total variance. The SPCZ position for El Niño (green line), La Niña (blue line) and neutral (black line) states is superimposed in **a**, and for zonal SPCZ events (red line) in **b**. The SPCZ position is defined as the position where the maximum rainfall greater than 6 mm per day[5] is situated and a linear fit is applied. **c,** A nonlinear relationship between the associated principal component time series. La Niña, neutral and moderate El Niño years are indicated with blue, black and green dots,

respectively. A zonal SPCZ event (red dots) is defined as when the first principal component is greater than one standard deviation, and when the second principal component is positive. The different phases of ENSO events (El Niño and La Niña) are determined from a detrended Niño3.4 index when its amplitude is greater than 0.5 of the standard deviation value.

Figure 2| Multi-model ensemble average of the principal variability patterns of rainfall and their nonlinear relationship from eight CMIP3 CGCMs that are able to produce the nonlinear relationship. **a**, **b**, The first and the second principal variability patterns. The multi-model composite SPCZ position over the full 200 years for El Niño (green), La Niña (blue) and neutral (black) states is superimposed in **a**, and for zonal SPCZ events (red) in **b**. **c, d,** The relationship between the associated two principal component time series for the *Control* (1891-1990) and *Climate Change* (1991-2090) periods from the eight CMIP3 CGCMs. La Niña, neutral and moderate El Niño years are indicated with blue, black and green dots, respectively. Variance accounted for by the first and second principal pattern is model-dependent and ranges from 40-53% and 8-15% of the total variance, respectively. An increase in zonal SPCZ events (red dots) from the *Control* to *Climate Change* period is evident from a comparison between **c** and **d**. An El Niño (La Niña) is defined as when the detrended index has an amplitude greater than a 0.5 standard deviation value.

Figure 3| Multi-model composites of the circulation fields associated with zonal SPCZ events. Shown are surface winds (m s^{-1}), SST (^{o}C), and rainfall (mm/day) anomalies referenced to the mean climate of the *Control* period. **a, b**, events over the *Control* period; and **c, d,** events over the *Climate Change* period. Contours of the composite 28^{o}C isotherm are superimposed on the SST anomalies (purple) and total rainfall at 6 mm per day (thick black contour) and 12 mm per day (thin black contour) are superimposed on the rainfall anomalies. The eight CMIP3 CGCM ensemble average shows a ~10% intensity rainfall increase over the SPCZ area during such zonal SPCZ events, from the *Control* period to the *Climate Change* period, and in areas confined by the green curve, statistically significant above the 95% confidence level based on a t-test comparing two averages.

Figure 4| Multi-model statistics associated with the increase in the frequency of zonal SPCZ events. a, Multi-model histogram of the meridional SST gradient in the central equatorial Pacific for the eight CMIP3 CGCMs that are able to produce the nonlinear relationship for the *Control* and *Climate Change* period. The meridional SST gradient is defined as the average SST over the off-equatorial region (10°S-5°S, 155°E-120°W) minus the average over the equatorial region (5°S-Eq., 155°E-120°W). All 800-years in each period are separated in 0.25°C bins centered at the tick point for the *Control* (blue) and *Climate Change* (red) period. The multi-model median meridional SST gradient for the *Control* (solid grey line) and the *Climate Change* (dashed grey line) periods are indicated. **b**, The same as **a** but for zonal SPCZ events only. Note, the horizontal axis in **a** and **b** are reversed. **c**, Changes in the number of austral summers in which the meridional SST difference virtually vanishes (i.e., < 0.25°C), with all eight CGCMs producing an increase**. d,** Changes in the number of strong El Niño (the Niño3.4 index greater than a 1.5 standard deviation value), with two CGCMs showing a decrease (UKMO-HadCM3 and GFDL-CM2.1).

METHODS

Selection of models. While most of the comprehensive CGCMs are able to simulate the climatological mean SPCZ position and the relationship between the SPCZ and ENSO[23], their ability to simulate the observed nonlinear relationship between the SPCZ and equatorial warming has not been assessed. An EOF analysis[24] is performed on full 200 years of austral summer rainfall anomaly data from each of the 17 CMIP3 CGCMs[12]. The name of each CGCM is detailed in Supplementary Table 1. Nine models fail to reproduce the observed feature in terms of a nonlinear relationship between EOF1 and EOF2 time series. These same nine models also poorly simulate the EOF2 pattern with contrasting anomalies over the equatorial western and central Pacific (Supplementary Fig. 2 and Table 1). We therefore focus on the remaining eight models that do reproduce the observed nonlinear behaviour. Out of the 35 CMIP5 experiments from 20 CGCMs (available at the time of writing), only eight CGCMs with a total of 15 experiments produce the nonlinear behaviour of the SPCZ (Supplementary Table 2). Likewise, out of 17 PPE experiments, only 12 CGCMs simulate the observed nonlinearity of the SPCZ. Outputs from all experiments run from 1891 to 2090, under historical anthropogenic and natural forcings and then

under projected climate scenarios. We derive changes in the occurrence of zonal SPCZ events by comparing the frequency of the first 100 years (*Control* period) from that of the second 100 years (*Climate Change* period) in CGCMs that are able to produce zonal SPCZ events.

Statistical significance test. We use a bootstrap method[26] to examine whether the change in frequency of the zonal SPCZ events is statistically significant. The 800-year samples from the eight CMIP3 CGCMs in the *Control* period are re-sampled randomly to construct another 5000 realisations of 800-year records. During the random re-sampling process, overlapping is allowed, so that any one zonal SPCZ event can be selected again. The standard deviation of the zonal SPCZ frequency in the inter-realisation is 7.4 events per 800 years, far smaller than the difference between the *Control* and the *Climate Change* periods at 48 events per 800 years. The maximum frequency is 86, far smaller than that in the *Climate Change* period, further highlighting the strong statistical significance of the difference between the two periods. Increasing the realisations to 10,000 yields an essentially identical result. This process is repeated for the 15 CMIP5 experiments to create 10,000 realisations of 1500 samples, and for the 12 PPE experiments to generate 10,000 realisations of 1200 samples, from their respective *Control* period. In both cases, the standard deviation of the zonal SPCZ frequency in the inter-realisation is far smaller that the difference between the *Climate Change* and *Control* period, while the maximum frequency of zonal SPCZ events is far smaller than that in the *Climate Change* period, indicating a strong statistical significance. The eight CMIP3 CGCM ensemble average shows a ~10% intensity rainfall increase over the SPCZ area, from the *Control* period to the *Climate Change* period (Figure 3d). We use a t-test to compare the two averages and to determine whether a statistically significance above the 95% confidence level is achieved.

Acknowledgements

This work is supported by the Australian Climate Change Science Program, CSIRO Office of Chief Executive Science Leader programme, and the Pacific-Australia

Climate Change Science and Adaptation Planning Program. A.T. and M.W. were supported by the Office of Science (BER) U.S. Department of Energy, Grants DE-FG02-07ER64469, the U.S. National Science Foundation under grant 1049219 and by the Japan Agency for Marine-Earth Science and Technology (JAMSTEC). M.J.M is supported by NOAA and by CSIRO as a visiting scholar. M.L., C.M. and E.M.V. were supported by the Institut de Recherche pour le Développement (IRD). PMEL contribution number 3830.

Author Contributions W.C. and M.L. contributed to the central idea and wrote the initial draft of the paper. S. Borlace performed data analyses. M. Collins conducted and analysed the perturbed physics ensemble climate change experiments with the HadCM3 model. All authors contributed to refining the idea, improving the method, interpreting mechanisms, and the writing of this paper.

Author information Correspondence and requests for materials should be addressed to Wenju Cai (wenju.cai@csiro.au)

Figures

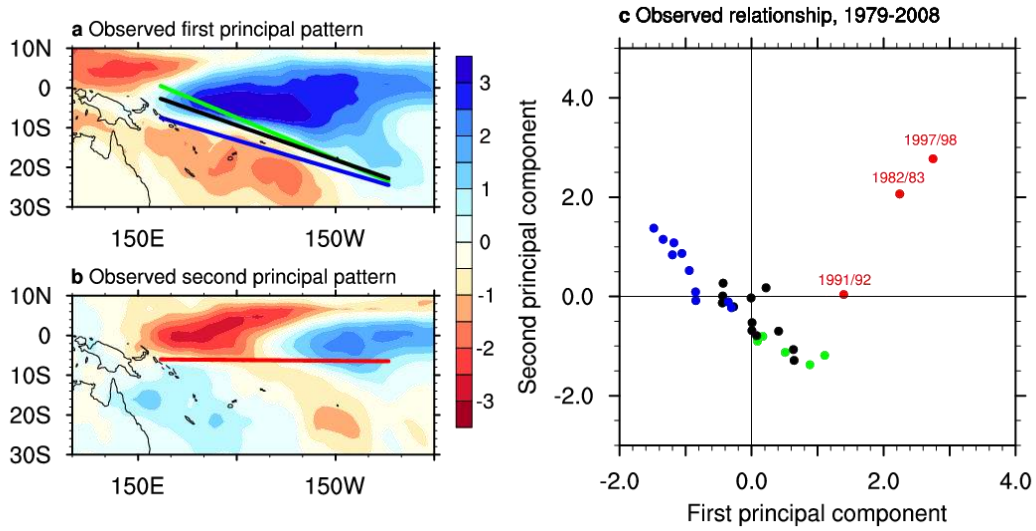

Figure 1| Principal variability patterns of observed rainfall and their nonlinear relationship. a and **b**, Spatial patterns obtained by applying a statistical and signal processing method, Empirical Orthogonal Function analysis[24], to a satellite-era rainfall dataset from the Global Precipitation Climatology Project version 2[25], focusing on the South Pacific domain (Eq.-30°S, 160°E-80°W) and the SPCZ prevailing season of austral summer (December to February). The associated pattern beyond the domain is obtained by linearly regressing rainfall anomalies onto the time series. The first and second principal spatial patterns account for 47% and 16% of the total variance. The SPCZ position for El Niño (green line), La Niña (blue line) and neutral (black line) states is superimposed in **a**, and for zonal SPCZ events (red line) in **b**. The SPCZ position is defined as the position where the maximum of rainfall greater than 6 mm per day[5] is situated and a linear fit is applied. **c,** A nonlinear relationship between the associated principal component time series. La Niña, neutral and moderate El Niño years are indicated with blue, black and green dots, respectively. A zonal SPCZ event (red dots) is defined as when the first principal component is greater than one standard deviation, and when the second principal component is positive. The different phases of ENSO events (El Niño and La Niña) are determined from a detrended Niño3.4 index when its amplitude is greater than 0.5 of the standard deviation value.

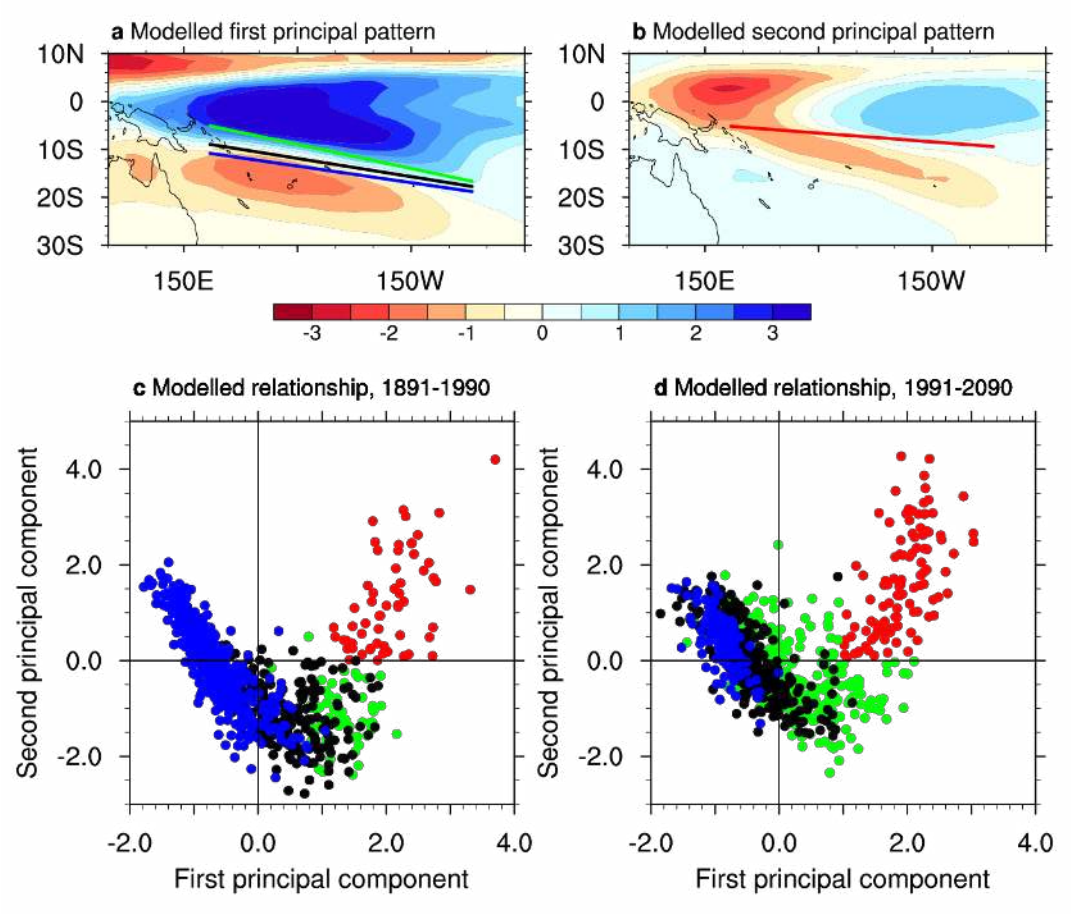

Figure 2| Multi-model ensemble average of the principal variability patterns of rainfall and their nonlinear relationship from eight CMIP3 CGCMs that are able to produce the nonlinear relationship. **a**, **b**, The first and the second principal variability patterns. The multi-model composite SPCZ position over the full 200 years for El Niño (green), La Niña (blue) and neutral (black) states is superimposed in **a**, and for zonal SPCZ events (red) in **b**. **c, d,** The relationship between the associated two principal component time series for the *Control* (1891-1990) and *Climate Change* (1991-2090) periods from the eight CMIP3 CGCMs. La Niña, neutral and moderate El Niño years are indicated with blue, black and green dots, respectively. Variance accounted for by the first and second principal pattern is model-dependent and ranges from 40-53% and 8-15% of the total variance, respectively. An increase in zonal SPCZ events (red dots) from the *Control* to *Climate Change* period is evident from a comparison between **c** and **d**. An El Niño (La Niña) is defined as when the detrended index has an amplitude greater than a 0.5 standard deviation value.

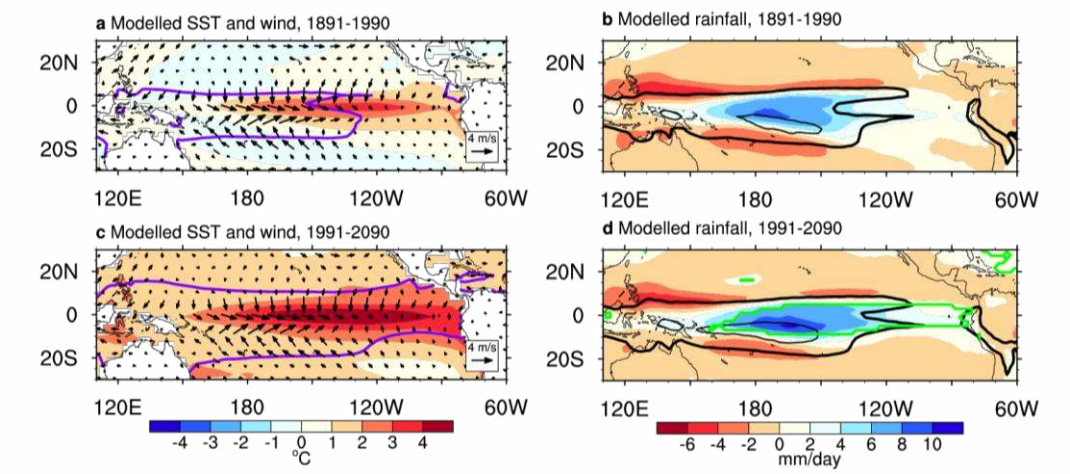

Figure 3| Multi-model composites of the circulation fields associated with zonal SPCZ events. Shown are surface winds (m s^{-1}), SST (^{o}C), and rainfall (mm/day) anomalies referenced to the mean climate of the *Control* period. **a, b**, events over the *Control* period; and **c, d,** events over the *Climate Change* period. Contours of the composite 28^{o}C isotherm are superimposed on the SST anomalies (purple) and total rainfall at 6 mm per day (thick black contour) and 12 mm per day (thin black contour) are superimposed on the rainfall anomalies. The eight CMIP3 CGCM ensemble average shows a ~10% intensity rainfall increase over the SPCZ area, from the *Control* period to the *Climate Change* period, and in areas confined by the green curve, statistically significant above the 95% confidence level based on a t-test comparing two averages.

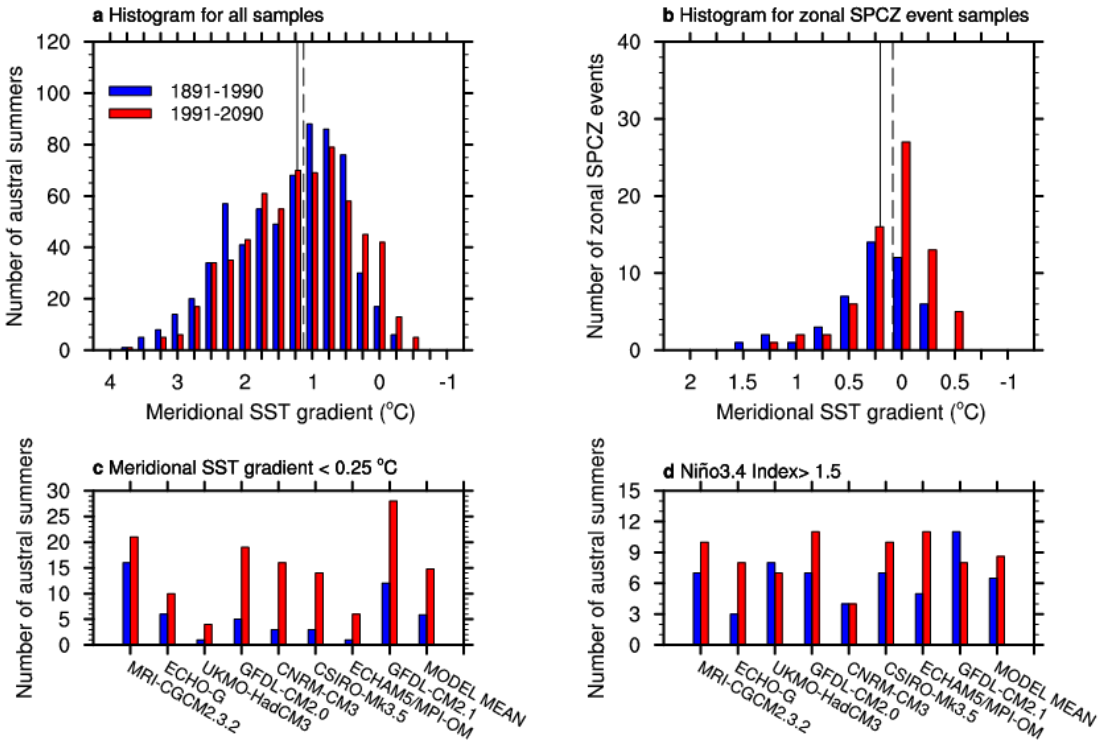

Figure 4| Multi-model statistics associated with the increase in the frequency of zonal SPCZ events. a, Multi-model histogram of meridional SST gradient in the central equatorial Pacific for the eight CMIP3 CGCMs that are able to produce the nonlinear relationship for the *Control* and *Climate Change* period. The meridional SST gradient is defined as the average SST over the off-equatorial region (10°S-5°S, 155°E-120°W) minus the average over the equatorial region (5°S-Eq., 155°E-120°W). All 800 years in each period are separated in 0.25°C bins centered at the tick point for the *Control* (blue) and *Climate Change* (red) period. The multi-model median meridional SST gradient for the *Control* (solid grey line) and the *Climate Change* (dashed grey line) periods are indicated. **b**, The same as **a** but for zonal SPCZ events only. Note, the horizontal axis in **a** and **b** are reversed. **c**, Changes in the number of austral summers in which the meridional SST difference virtually vanishes (i.e., < 0.25°C), with all eight CGCMs producing an increase**. d,** Changes in the number of strong El Niño (the Niño3.4 index greater than a 1.5 standard deviation value), with two CGCMs showing a decrease (UKMO-HadCM3 and GFDL-CM2.1).

Supplementary material for
More extreme swings of the South Pacific Convergence Zone due to greenhouse warming

Wenju Cai[1], Matthieu Lengaigne[2], Simon Borlace[1], Mat Collins[3], Tim Cowan[1], Michael J. McPhaden[4], Axel Timmermann[5], Scott Power[6], Josephine Brown[6], Christophe Menkes[7], Arona Ngari[8], Emmanuel M. Vincent[2], and Matthew Widlansky[9]

1. CSIRO Marine and Atmospheric Research, Australia
2. Laboratoire d'Océanographie et du Climat: Expérimentation et Approches Numériques (LOCEAN), IRD/UPMC/CNRS/MNHN, Paris, France
3. College of Engineering Mathematics and Physical Sciences, Harrison Building, Streatham Campus, University of Exeter, Exeter, UK and Met Office Hadley Centre, FitzRoy Road, Exeter, EX1 3PB, UK,
4. NOAA/Pacific Marine Environmental Laboratory, Seattle, Washington 98115, USA
5. IPRC, Department of Oceanography, SOEST, University of Hawaii, Honolulu, Hawaii 96822, USA
6. Centre for Australian Weather and Climate Research, Bureau of Meteorology, Melbourne, Victoria, Australia
7. Institut de Recherche pour le Développement, Noumea, New Caledonia
8. Meteorological Service, Avarua, Rarotonga, Cook Islands
9. International Pacific Research Center, University of Hawaii at Manoa, Honolulu, Hawaii 96822, USA

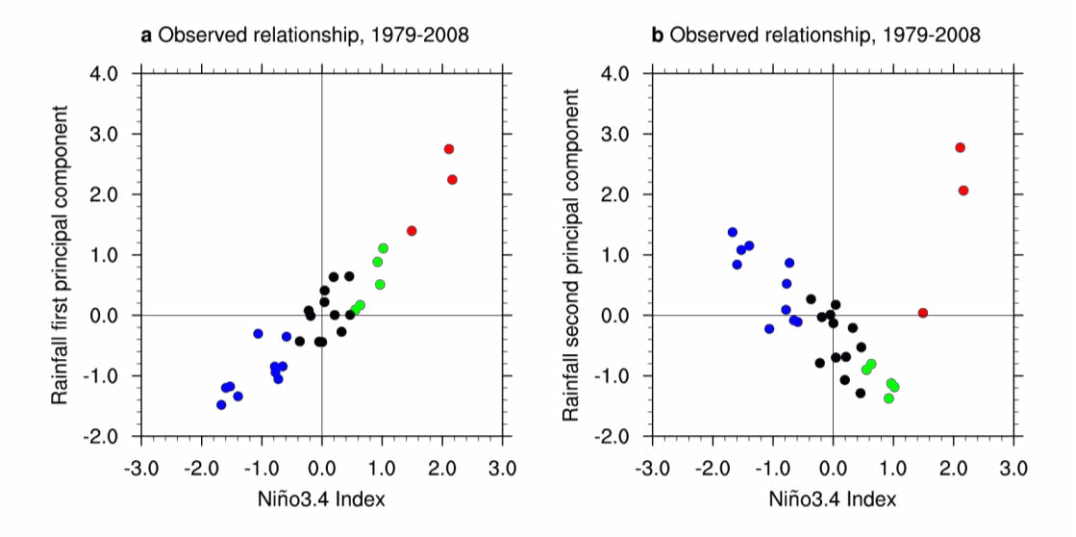

Supp. Figure 1 | Relationship between leading time series of observed rainfall[1] variability and ENSO. ENSO is represented by a normalised Niño3.4 index (SST anomaly averaged over 5°N-5°S, 120°W-170°W, commonly used to characterize the occurrence of El Niño and La Niña) based on HadISST[2], for **a** the first leading and **b** the second leading pattern. Red dots represent zonal SPCZ events. La Niña, neutral and moderate El Niño years are indicated with blue, black and green dots, respectively.

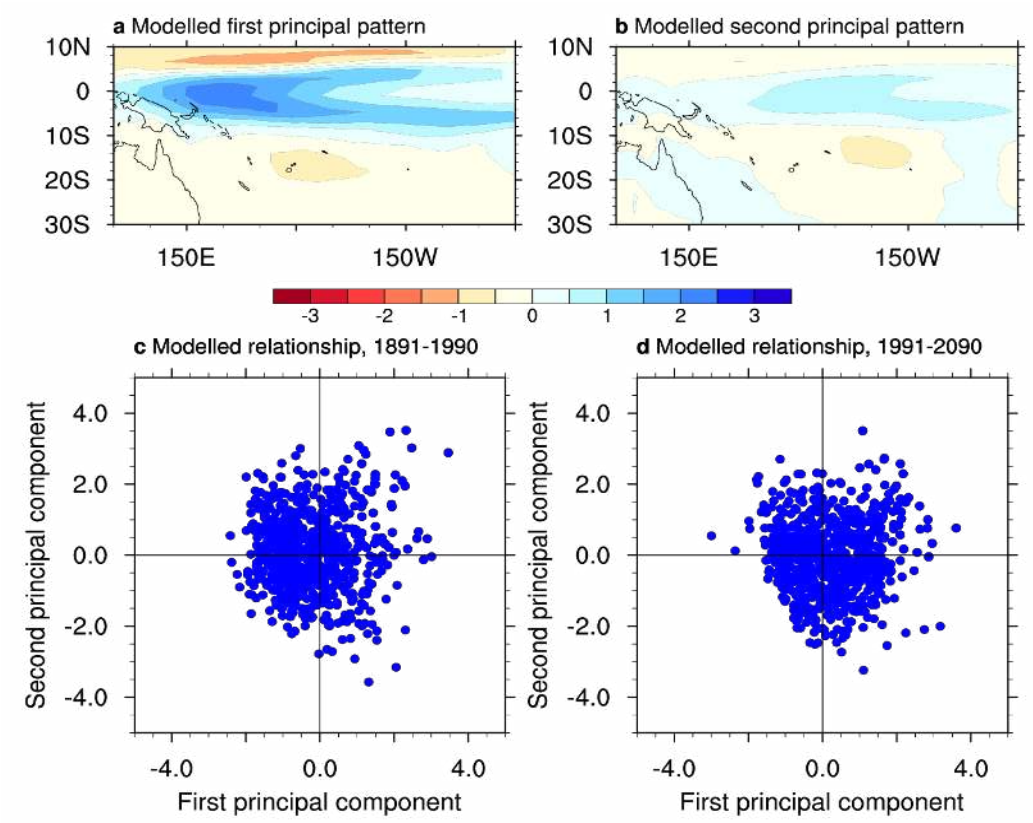

Supp. Figure 2| Multi-model ensemble average of the leading variability patterns of rainfall and their relationship for the nine CMIP3 CGCMs that are NOT able to produce the nonlinear relationship (see Supp. Table 1). a, b, The leading first and second preferred rainfall variability patterns. In the second pattern these nine CGCMs do not have a well-defined east-west contrast. **c, d,** Relationship between the two associated leading time series for the *Control* (1891-1990) and *Climate Change* periods from nine CGCMs (1991-2090). Note the absence of a nonlinear relationship in **c** and **d**.

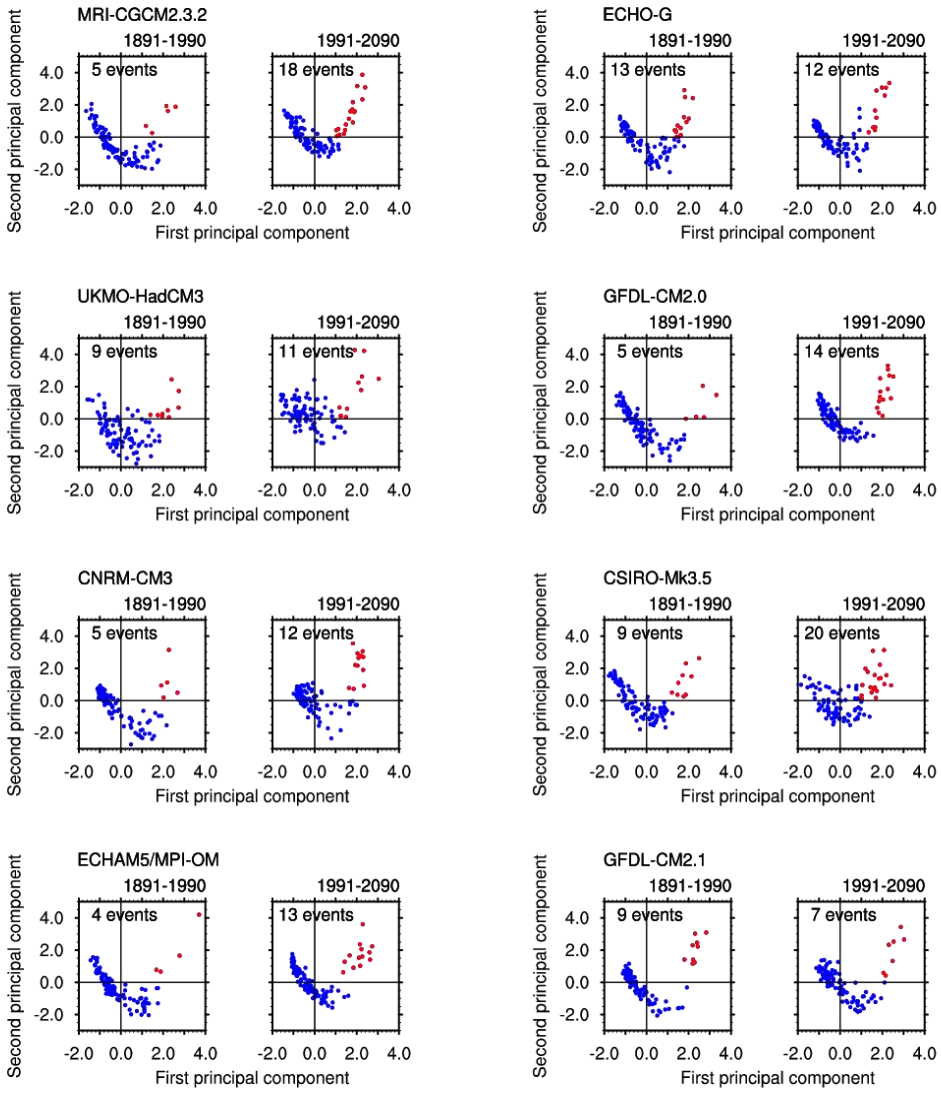

Supp. Figure 3| Performance of the eight CMIP3 CGCMs that simulate the nonlinear behaviour of the SPCZ. Shown for the 100-year *Control* (1891-1990) and *Climate Change* (1991-2091) periods. Red dots represent zonal SPCZ events, defined as when the second principal component time series is greater than zero and the first principal component time series is greater than one standard deviation. In most CGCMs, the second principal component time series trends up, leading to an increase in zonal SPCZ events.

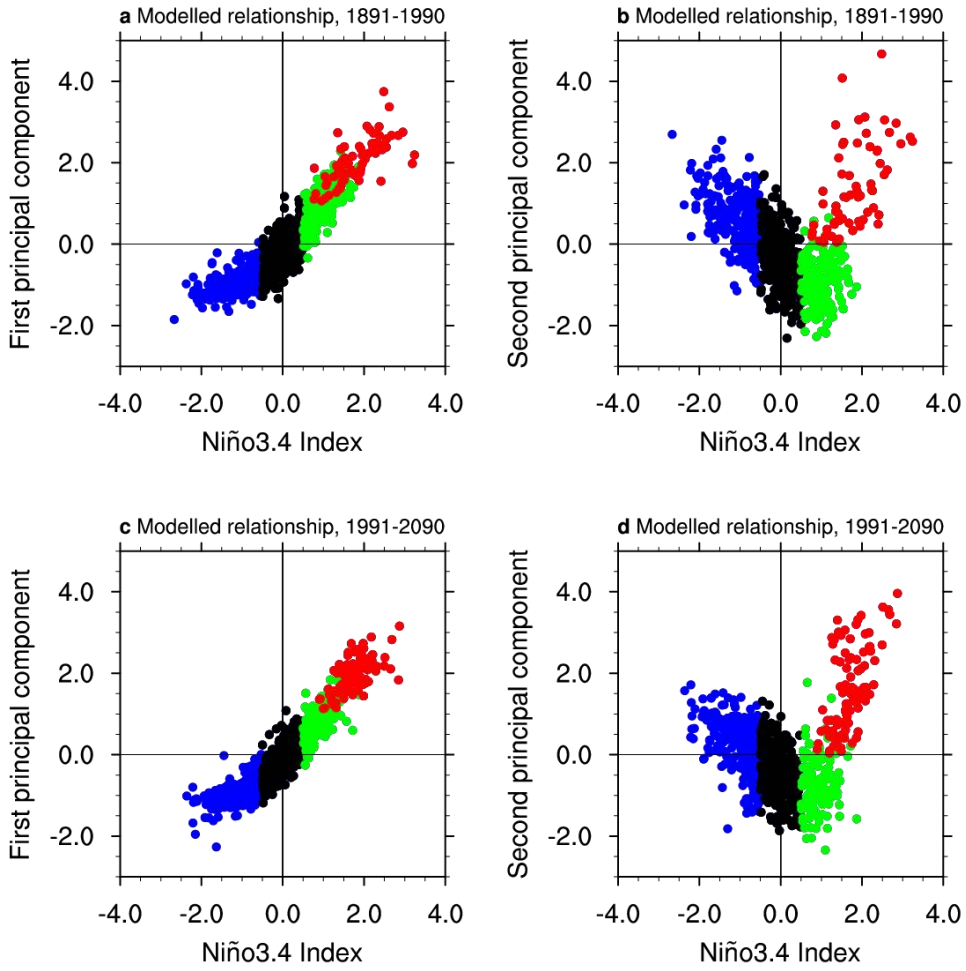

Supp. Figure 4. Relationship between the leading two principal components and the Niño3.4 index. **a** and **b** for the *Control* period, and **c** and **d** for the *Climate Change* period for CMIP3 CGCMs that are able to produce the nonlinear relationship between the first and second leading time series. Red dots represent zonal SPCZ events. The main results to highlight are the linear relationship of the detrended Niño3.4 index with the first EOF and the nonlinear relationship with the second EOF. These relationships continue as global warming proceeds. SST anomalies over the Niño3.4 region are referenced to the mean over the 200 years, and are detrended using a quadratic fit over the 200-year period. La Niña, neutral and moderate El Niño years are indicated with blue, black and green dots, respectively.

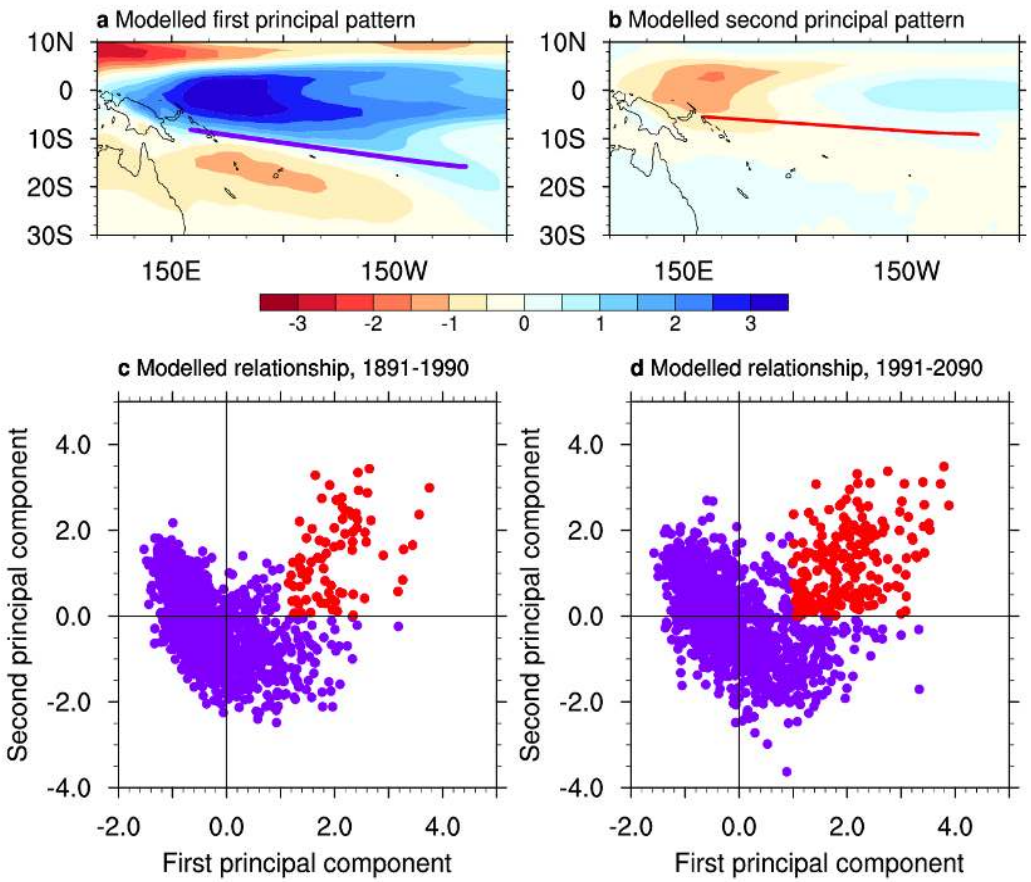

Supp. Figure 5. Multi-model ensemble average of principal variability patterns of rainfall and their nonlinear relationship from 15 experiments from eight CMIP5 CGCMs that are able to produce the nonlinear relationship (see Supp. Table 2). **a, b,** The first and the second principal variability patterns. The multi-model composite position is shown for non-zonal (purple line in **a**) and zonal (red line in **b)** SPCZ events. The SPCZ position is defined as the position where maximum rainfall greater than 6 mm per day is situated. At the time of writing, no data was available to stratify into El Niño and La Niña events. **c, d,** Relationship between the associated two principal component time series for the *Control* (1891-1990) and *Climate Change* (1991-2090) periods. An increase in zonal SPCZ events (red dots) from the *Control* to *Climate Change* period is evident from a comparison between **c** and **d.**

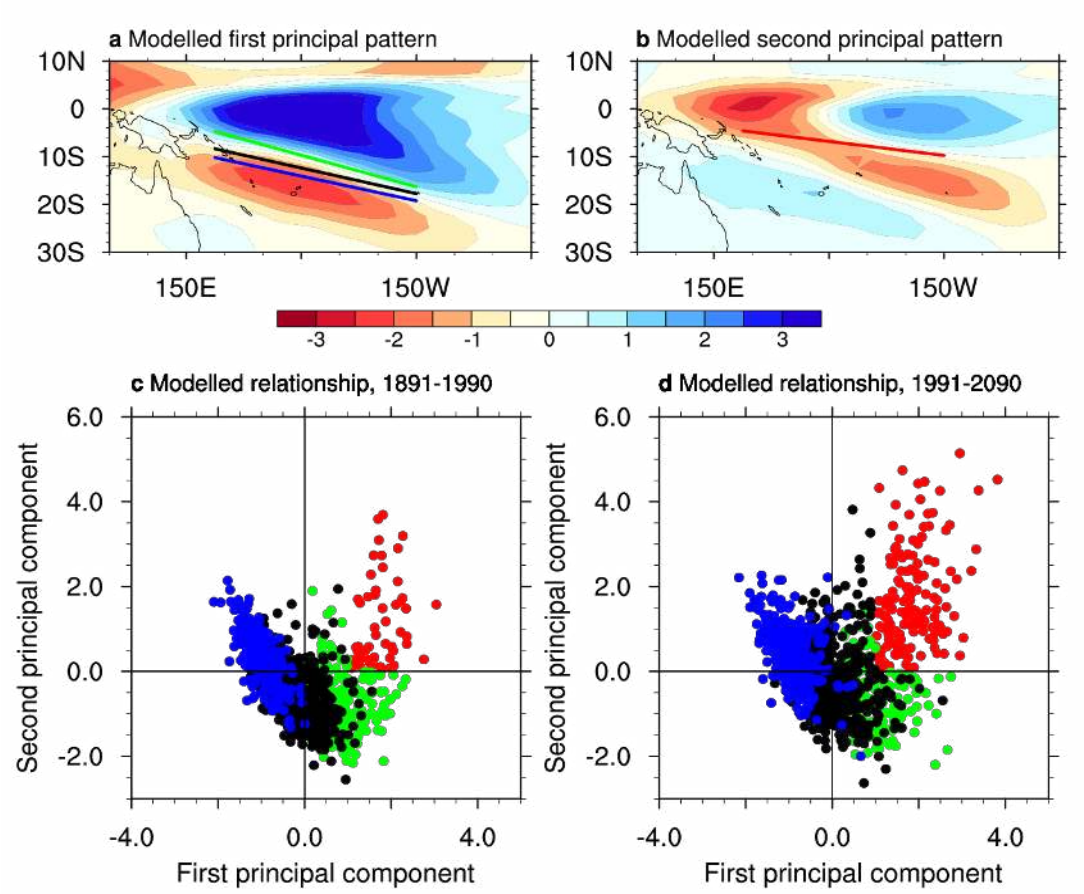

Supp. Figure 6 | Multi-member ensemble average of the principal variability patterns of rainfall and their nonlinear relationship. Shown are from 12 HadCM3 flux-adjusted PPE experiments[4,5] that are able to produce the nonlinear behaviour of the SPCZ. **a**, **b**, The first and the second principal variability patterns. The multi-model composite SPCZ position over the full 200 years for El Niño (green), La Niña (blue) and neutral (black) states is superimposed in **a**, and for zonal SPCZ (red) in **b**. The SPCZ position is defined as the position where maximum rainfall is greater than 6 mm per day. El Niño and La Niña events are determined from a Niño3.4 index, nonlinearly detrended following a quadratic fit. An El Niño (La Niña) is defined as when the detrended Niño3.4 index has an amplitude greater than a 0.5 standard deviation value. **c, d**, Relationship between the associated two principal component time series for the *Control* (1891-1990) and *Climate Change* (1991-2090) periods from the 12 PPE experiments. An increase in zonal SPCZ events (red dots) from 57 events in the *Control* to 179 events in the *Climate Change* period is evident from a comparison between **c** and **d (see Supplementary Table 3)**.

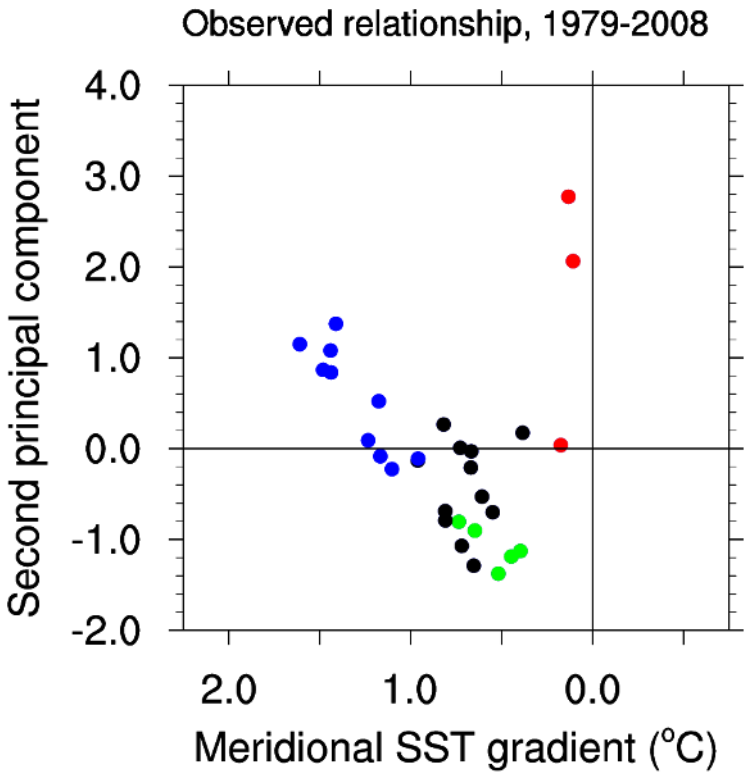

Supp. Figure 7 | Relationship between the second principal component time series of observed rainfall[1], which describes the east-west pattern of SPCZ variability, and a meridional SST gradient in the central equatorial Pacific. Red dots represent zonal SPCZ events. The meridional SST gradient is calculated as SST averaged over the off-equatorial region (10°S-5°S, 155°E-120°W) minus SST averaged over the equatorial region (5°S-Eq., 155°E-120°W). Note the nonlinear relationship of the second principal component time series with the meridional SST gradient. La Niña, neutral and moderate El Niño years are indicated with blue, black and green dots, respectively.

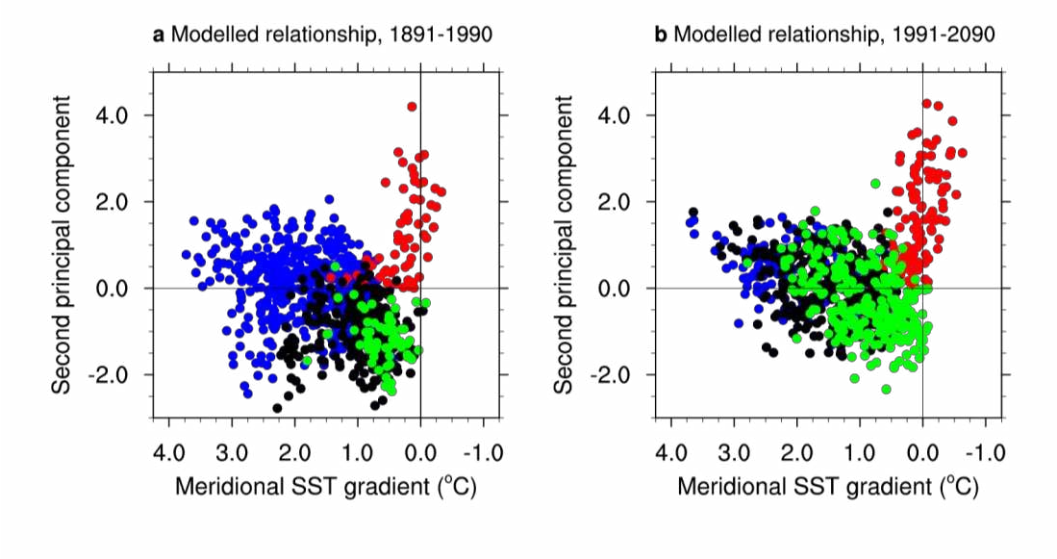

Supp. Figure 8 | CMIP3 multi-model ensemble relationship between the second principal component time series, which describes the east-west pattern of SPCZ variability, and a meridional SST gradient in the central equatorial Pacific. **a** the *Control* period, and **b** the *Climate Change* period. This is for the eight CGCMs that are able to produce the nonlinear behaviour of the SPCZ. Red dots represent zonal SPCZ events. The meridional SST gradient is calculated as SST averaged over the off-equatorial region (10°S-5°S, 155°E-120°W) minus SST averaged over the equatorial region (5°S-Eq., 155°E-120°W). Note the nonlinear relationship of the second principal component time series with the meridional SST gradient that continues as global warming proceeds. Zonal SPCZ events tend to occur when the meridional gradient is small, and occur more frequently in the *Climate Change* period. La Niña, neutral and moderate El Niño years are indicated with blue, black and green dots, respectively.

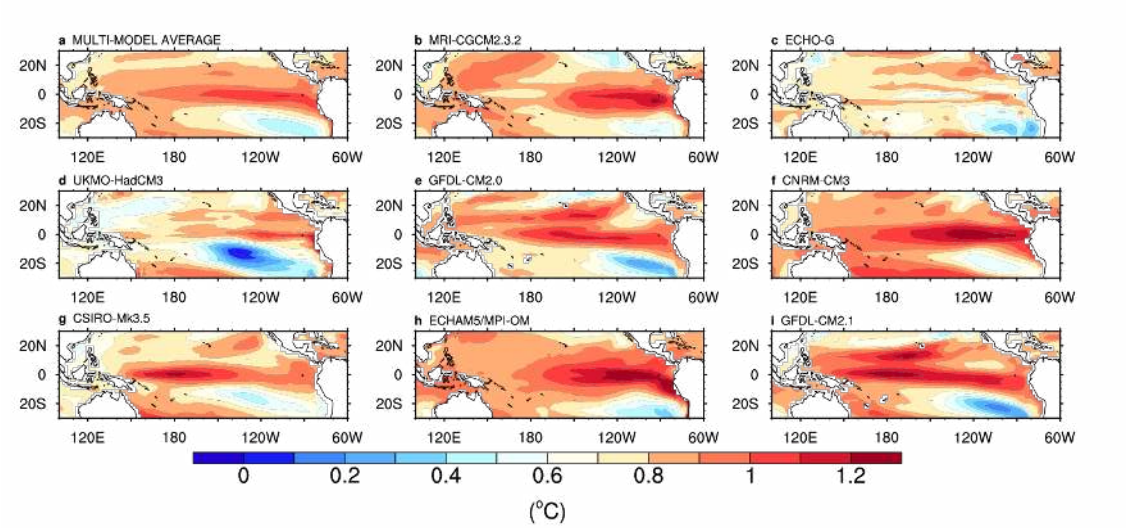

Supp. Figure 9 | Changes in SST in the *Climate Change* period (°C per °C of global warming) in CMIP3 CGCMs. **a**, Multi-model ensemble average; **b-i,** for each of the eight individual models. These are obtained for each model by linearly regressing SST onto global mean surface temperature. The majority of the models show a faster warming rate on the equator than in the off-equatorial regions[6], forcing the warm pool to be more zonally oriented, and decreasing the meridional SST gradient in the central equatorial Pacific.

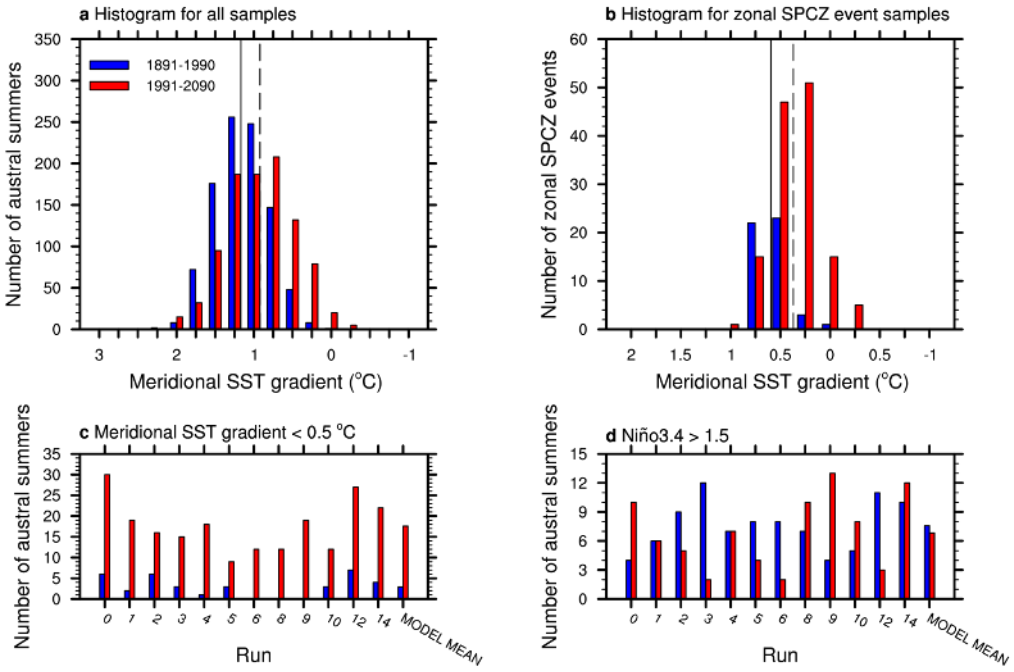

Supp. Figure 10 | HadCM3 flux-adjusted PPE experiment statistics associated with the increase in the frequency of zonal SPCZ events. **a**, Multi-model histogram of meridional SST gradient in the central equatorial Pacific for the eight CMIP3 CGCMs that are able to produce the nonlinear relationship for the *Control* and *Climate Change* period. The meridional SST gradient is defined as the average SST over the off-equatorial region (10°S-5°S, 155°E-120°W) minus the average over the equatorial region (5°S-Eq., 155°E-120°W). All 800-years in each period are separated in 0.25°C bins centered at the tick point for the *Control* (blue) and *Climate Change* (red) period. The multi-model median meridional SST gradient for the *Control* (solid grey line) and the *Climate Change* (dashed grey line) period are indicated. **b**, The same as **a** but for zonal SPCZ events only. Note the horizontal axis is reversed in **a** and **b**. **c** and **d,** Changes in the number of austral summers in which the meridional SST difference virtually vanishes (i.e., < 0.5°C, as opposed to 0.25°C in CMIP3 eight CGCMs, to capture most zonal SPCZ events), and an El Niño greater than a 1.5 standard deviation value.

Supp. Table 1. Performance of 17 CGCMs submitted to CMIP3 forced with climate change emission scenario A2[7]. This is examined in terms of each model's ability to simulate the nonlinear behaviour of the SPCZ (column 2). Sensitivity of changes in zonal SPCZ events from the *Control* to *Climate Change* period to different definitions is tested. A zonal SPCZ event is defined as when the second principal component time series is greater than 0 and the first principal component time series is greater than 0.5 (EOF1>0.5, column 3) or 1.0 (EOF1>1, column 4) standard deviation value. ENSO amplitude (column 5) is defined as the standard deviation of the detrended Niño3.4 index using a quadratic fit over the full 200-year period. Models that are able to produce the nonlinear relationship tend to have a greater ENSO amplitude and more realistic teleconnection[8]. Numbers in bold indicate an increase from the *Control* period. There is no consensus on the direction of change in ENSO amplitude. A bootstrap test shows that the change in zonal SPCZ events in GFDL-CM2.1, MIUB-ECHO.g, and UK-HadCM3 is smaller than the standard deviation of inter-realisation variations from 500 sets of 100-year records re-sampled from the *Control* period. In all other models, the change is greater than the standard deviation of the corresponding inter-realisation variations.

CGCM	SPCZ nonlinear behaviour	Zonal SPCZ Events (EOF1> 0.5 Standard Deviation and EOF2 > 0) (1891-1990)/ (1991-2090)	Zonal SPCZ Events (EOF1> 1.0 Standard Deviation and EOF2 > 0) (1891-1990)/ (1991-2090)	ENSO Amplitude (°C) (1891-1990)/ (1991-2090)
GISS-ER	No			0.21/0.21
UKMO-HadGEM1	No			0.62/**0.85**
MIROC3.2(medres)	No			0.55/0.51
PCM	No			0.92/0.74
INGV-SXG	No			0.87/**0.90**
CCSM3	No			1.01/0.87
CSIRO-Mk3.0	No			0.89/**0.90**
IPSL-CM4	No			1.15/1.05
INM-CM3.0	No			0.77/**0.78**
MRI-CGCM2.3.2	Yes	5 /**18**	5 /**18**	0.82/**1.25**
ECHO-G	Yes	13/**16**	13/12	1.31/1.20
UKMO-HadCM3	Yes	11/**14**	9 /**11**	1.16/1.16
GFDL-CM2.0	Yes	5 /**14**	5 /**14**	1.11/**1.44**
CNRM-CM3	Yes	5 /**12**	5 /**12**	1.92/1.77
CSIRO-Mk3.5	Yes	9 /**26**	9 /**20**	1.06/0.99
ECHAM5/MPI-OM	Yes	4 /**13**	4 /**13**	1.43/**1.65**
GFDL-CM2.1	Yes	9 / 7	9 /7	1.65/1.53
Total and % change between the two periods		61/**120 (96%)**	59 /**107 (81%)**	

Supp. Table 2. Changes in the frequency of zonal SPCZ events from the *Control* to *Climate Change* period in 15 experiments from eight CMIP5 CGCMs that are able to simulate the nonlinear behaviour of the SPCZ. Sensitivity of changes to different definitions is tested. Numbers in bold indicate an increase from the *Control* period. A zonal SPCZ event is defined as when the second principal component time series is greater than 0 and the first principal component time series is greater than a 0.5 (EOF1> 0.5) or 1.0 (EOF1> 1) standard deviation value. For the latter definition, 15 experiments produce an increase of 111%.

CMIP5 CGCM and Experiment		Zonal SPCZ Events (EOF1> 0.5 Standard Deviation and EOF2 > 0) (1891-1990)/ (1991-2090)	Zonal SPCZ Events (EOF1> 1 Standard Deviation and EOF2 > 0) (1891-1990)/ (1991-2090)
CCSM4	Run1	9/6	9/6
	Run2	9/**11**	7/**10**
	Run3	13/11	9/**11**
CNRM-CM5	Run1	12/**16**	12/**16**
	Run2	10/**16**	10/**16**
CSIRO-Mk3.6	Run1	1/**27**	1/**24**
	Run2	0/**25**	0/**19**
	Run3	1/**27**	1/**24**
FGOALS-g2	Run1	18/**20**	14/13
GFDL-CM3	Run1	10/10	7/**9**
GFDL-ESM2M	Run1	11/8	11/8
MIROC5	Run1	4/**8**	4/**7**
	Run2	1/**11**	1/**11**
	Run3	4/**12**	4/**11**
MRI-CGCM3	Run1	5/**21**	5/**16**
Total and % change between the two periods		108/**229 (112%)**	95/**201 (111%)**

Supp. Table 3. The same as Supp. Table 1, but for 17 PPE climate change experiments forced with a 1% per year CO_2 increase using HadCM3 CGCM in which biases are corrected through a fixed flux adjustment. All 12 model versions that are able to produce the nonlinear behaviour show an increase in the occurrences of zonal SPCZ events, and in aggregation there is a 214% increase for the definition discussed in the text**.**

CGCM	SPCZ nonlinear behaviour	Zonal SPCZ Events (EOF1> 1 Standard Deviation and EOF2 > 0) (1891-1990)/ (1991-2090)	Zonal SPCZ Events (EOF1> 0.5 Standard Deviation and EOF2 > 0) (1891-1990)/ (1991-2090)	ENSO Amplitude (^{o}C) (1891-1990)/ (1991-2090)
Run 0	Yes	3/**14**	3/**18**	0.71/**1.02**
Run 1	Yes	6/**18**	7/**22**	0.89/**0.94**
Run 2	Yes	7/**12**	9/**16**	0.86/0.85
Run 3	Yes	9/**16**	12/**22**	0.73/0.57
Run 4	Yes	2/**15**	4/**16**	0.69/**0.89**
Run 5	Yes	7/**11**	10/**17**	0.88/0.84
Run 6	Yes	4/**17**	4/**17**	0.50/0.45
Run 7	No			0.41/**0.43**
Run 8	Yes	6/**16**	9/**20**	0.50/**0.61**
Run 9	Yes	0/**13**	0/**13**	0.52/**0.82**
Run 10	Yes	3/**14**	7/**17**	0.69/**0.87**
Run 11	No			0.43/**0.51**
Run 12	Yes	7/**18**	8/**25**	0.77/0.72
Run 13	No			0.39/**0.49**
Run 14	Yes	3/**15**	4/**22**	0.73/**0.77**
Run 15	No			0.42/**0.48**
Run16	No			0.65/0.65
Total and % change between the two periods		57/**179 (214%)**	77/**226 (193%)**	

Supp. Table 4. Changes in the frequency of El Niño and zonal SPCZ events in the eight CMIP3 CGCMs that are able to produce the nonlinear behaviour of the SPCZ. Sensitivity to definitions of an El Niño event is tested using the detrended Niño3.4 index (SST averaged over 5°S-5°N, 170°W-120°W) following a quadratic fit over the full 200-year period. Three definitions are used: Niño3.4 is greater than 0.5, 0.75, and 1.5 of a one standard deviation value. The number of zonal SPCZ events that occur with an El Niño is shown in bracket. Numbers in bold indicate an increase from the *Control* period. Although there is a tendency for a decrease in the total number of El Niño events (e.g. greater than a 0.5 standard deviation value), 5 out of the 8 models show an increase in strong El Niño events. Over 95% of such strong El Niño events lead to a zonal SPCZ event in the *Climate Change* period, compared to 79% in the *Control* period (Supplementary Table 3). However, there is an increase of only 25 zonal SPCZ events that occur with a strong El Niño event (Niño3.4 greater than 1.5 standard deviation), which accounts for about 50% of the total increase in zonal SPCZ events.

CGCM	Niño3.4 > 0.5 Standard Deviation Number of El Niño (Zonal SPCZ within El Niño) Events		Niño3.4 > 0.75 Standard Deviation Number of El Niño (Zonal SPCZ within El Niño) Events		Niño3.4 > 1.5 Standard Deviation Number of El Niño (Zonal SPCZ within El Niño) Events	
	1891-1990	1991-2090	1891-1990	1991-2090	1891-1990	1991-2090
MRI-GCM2.3.2	29 (5)	27 **(18)**	21 (5)	**22 (17)**	7 (4)	**10 (10)**
ECHO-G	38 (12)	34 (12)	33 (12)	27 (12)	3 (3)	**8 (7)**
UKMO-HadCM3	32 (9)	29 **(11)**	26 (9)	24 **(11)**	8 (7)	7 (7)
GFDL-CM2.0	28 (5)	24 **(14)**	22 (5)	19 **(14)**	7 (5)	**11 (11)**
CNRM-CM3	35 (5)	31 **(12)**	33 (5)	24 **(12)**	4 (3)	4 (3)
CSIRO-Mk3.5	27 (9)	27 **(19)**	16 (9)	**19 (17)**	7 (6)	**10 (10)**
ECHAM5/MPI-OM	29 (4)	27 **(13)**	28 (4)	20 **(13)**	5 (4)	**11 (11)**
GFDL-CM2.1	21 (9)	**27** (7)	16 (9)	**24** (7)	11 (9)	8 (7)
Total	239 (58)	226 **(106)**	195 (58)	179 **(103)**	52 (41)	**69 (66)**
Aggregated % Change from 1891-1990 to 1991-2090	-5.4% (**82.7%**)		-8.2% **(77.5%)**		**32.6% (60.9%)**	
% of Zonal SPCZ Events within El Niño Events	24.2%	**46.9%**	29.7%	**57.5%**	78.8%	**95.6%**

Supp. Table 5. Changes in the frequency of El Niño and zonal SPCZ events in 12 PPE climate change experiments that are able to produce the nonlinear behaviour of the SPCZ. These experiments are forced with a 1% per year CO_2 increase using the HadCM3 CGCM in which biases are corrected through a fixed flux adjustment. Sensitivity to definitions of an El Niño event is tested using the detrended Niño3.4 index (SST averaged over 5^oS-5^oN, 170^oW-120^oW) following a quadratic fit over the full 200-year period. Three definitions are used: Niño3.4 is greater than 0.5, 0.75, and 1.5 of a one standard deviation value. The number of zonal SPCZ events that occur with an El Niño is shown in brackets. Numbers in bold indicate an increase from the *Control* period. Although there is a tendency for an increase in the total number of El Niño events (e.g. greater than 0.5 standard deviation), there is no consensus on a change in strong El Niño events.

HadCM3 PPE	Niño3.4 > 0.5 Standard Deviation Number of El Niño (Zonal SPCZ) Events		Niño3.4 > 0.75 Standard Deviation Number of El Niño (Zonal SPCZ) Events		Niño3.4 > 1.5 Standard Deviation Number of El Niño (Zonal SPCZ) Events	
	1891-1990	1991-2090	1891-1990	1991-2090	1891-1990	1991-2090
Run 0	26 (3)	**35 (14)**	20 (3)	**29 (14)**	4 (3)	**10 (4)**
Run 1	32 (6)	**35 (15)**	27 (6)	26 **(14)**	6 (5)	**6 (4)**
Run 2	27 (7)	**33 (12)**	20 (7)	**24 (12)**	9 (5)	5 (4)
Run 3	33 (9)	25 **(14)**	26 (9)	21 **(14)**	12 (9)	2 (2)
Run 4	28 (2)	**35 (15)**	18 (2)	**28 (12)**	7 (2)	7 **(4)**
Run 5	33 (7)	29 **(10)**	25 (7)	**26 (10)**	8 (6)	4 (3)
Run 6	34 (4)	31 **(11)**	28 (4)	23 **(9)**	8 (4)	2 (1)
Run 8	30 (5)	28 **(14)**	22 (5)	**21(13)**	7 (4)	**10 (8)**
Run 9	22 (0)	**38 (13)**	14 (0)	**29 (12)**	4 (0)	**13 (7)**
Run 10	31 (3)	30 **(14)**	24 (3)	**25 (12)**	5 (2)	**8 (7)**
Run 12	26 (7)	**36 (14)**	22 (7)	**26 (13)**	11 (5)	3 (3)
Run 14	28 (3)	**29 (15)**	23 (3)	**26 (15)**	10 (3)	**12 (7)**
Total	350 (56)	**384 (161)**	269 (56)	**304 (150)**	91 (48)	82 **(54)**
% Change from 1891-1990 to 1991-2090	**9.7% (187.5%)**		**13.0% (167.9%)**		-9.9% (**12.5%**)	
% of Zonal SPCZ Events over El Niño Events	16.0%	**41.9%**	20.8%	**49.3%**	52.8%	**65.9%**

References

1. Adler, R. F. *et al*. The version 2 Global Precipitation Climatology Project (GPCP) monthly precipitation analysis (1979-present). *J. Hydrometeor*. **4**, 1147–1167 (2003).
2. Rayner, N. A. *et al*. Global analyses of sea surface temperature, sea ice, and night marine air temperature since the late nineteenth century. *J. Geophys. Res.* **108**, 4407, (2003).
3. Liebmann, B. & Smith, C. A. Description of a complete (interpolated) outgoing longwave radiation dataset. *Bull. Amer. Meteor. Soc.* **77**, 1275–1277 (1996).
4. Collins, M. *et al*. The impact of global warming on the tropical Pacific Ocean and El Niño. *Nature Geoscience* **3**, 391 - 397 (2010).
5. Collins, M. *et al*. A comparison of perturbed physics and multi-model ensembles: Model errors, feedbacks and forcings. *Clim. Dyn.* **36**, 1737-1766. (2011).
6. Xie, S. P. *et al*. Global Warming Pattern Formation: Sea Surface Temperature and Rainfall. *J. Clim.* **23**, 966-986 (2010).
7. Meehl, G. *et al*. The WCRP CMIP3 multimodel Dataset: A New Era in Climate Change Research. *Bull. Amer. Meteor. Soc.* **88**, 1383-1394 (2007).
8. Cai, W., Sullivan, A. & Cowan T. Rainfall teleconnections with Indo-Pacific variability in the IPCC AR4 models. *J. Clim.* **22**, 5046–5071 (2009).